Icarus **155**, 220–228 (2002)
doi:10.1006/icar.2001.6772, available online at http://www.idealibrary.com on IDEAL®

NEAR Magnetic Field Observations at 433 Eros: First Measurements from the Surface of an Asteroid

M. H. Acuña

NASA Goddard Space Flight Center, Greenbelt, Maryland 20771

B. J. Anderson

Applied Physics Laboratory, The Johns Hopkins University, Laurel Maryland 20723
E-mail: brian.anderson@jhuapl.edu

C. T. Russell

Institute of Geophysics and Planetary Physics, University of California, Los Angeles California 90095

P. Wasilewski and G. Kletetshka

NASA Goddard Space Flight Center, Greenbelt, Maryland 20771

L. Zanetti

Institute of Geophysics and Planetary Physics, University of California, Los Angeles, California 90095

and

N. Omidi

Department of Electrical and Computer Engineering, University of California San Diego, La Jolla California 92093

Received July 24, 2001; revised October 23, 2001

The magnetometer investigation aboard the NEAR-Shoemaker spacecraft has obtained extensive magnetic field observations throughout the 433 Eros environment, from distances in excess of 100,000 km to those conducted after landing on 12 February 2001. We report the apparent absence of global scale magnetization at this asteroid ($H < 0.005$ A · m^{-1}; natural remanent magnetization per kilogram $< 1.9 \times 10^{-6}$ A · m^2 · kg^{-1}), orders of magnitude less than the intense magnetization attributed to S-class asteroids Gaspra and Braille. The extremely low magnetization state of 433 Eros places this object significantly below the levels generally associated with LL chondrites and undifferentiated primitive bodies, challenging our current understanding of the meteorite–asteroid connection.

Key Words: **asteroids; Eros; magnetic fields.**

1. INTRODUCTION

The primary science objective of the NEAR-Shoemaker magnetic field investigation (MAG) was to characterize the magnetic field of Asteroid 433 Eros by direct measurements. It is generally accepted that asteroids are the parent bodies for most meteorites reaching the Earth (Wasson and Wetherill 1979, Feierberg *et al*. 1982). Compositional differences observed in meteorites are expected to reflect that of asteroids. The two basic groups that characterize meteorites, undifferentiated and differentiated, presumably reflect the thermal history of their parent bodies. Thus, ordinary chondrites are undifferentiated conglomerates of primitive material and contain intermixed grains of olivine, pyroxene, feldspar, and metallic Fe, reflective of the composition of the parent bodies. However, no unambiguous determination of the origin of ordinary chondrites has been made nor have the fundamental relationships between meteorites and asteroids been established. Gaffey *et al*. (1993) have stated that "the apparent paradox between the meteoritic and the asteroid evidence concerning the origin of the ordinary chondrites is one of the most important and perplexing problems in planetary science."

The NEAR MAG investigation and mission design were uniquely suited to mapping Fe-rich materials *in situ*, presuming the existence of a detectable asteroidal magnetic field. The Fe content of undifferentiated meteorites is expected to be in the form of randomly oriented fine grains with strong

0019-1035/02 $35.00

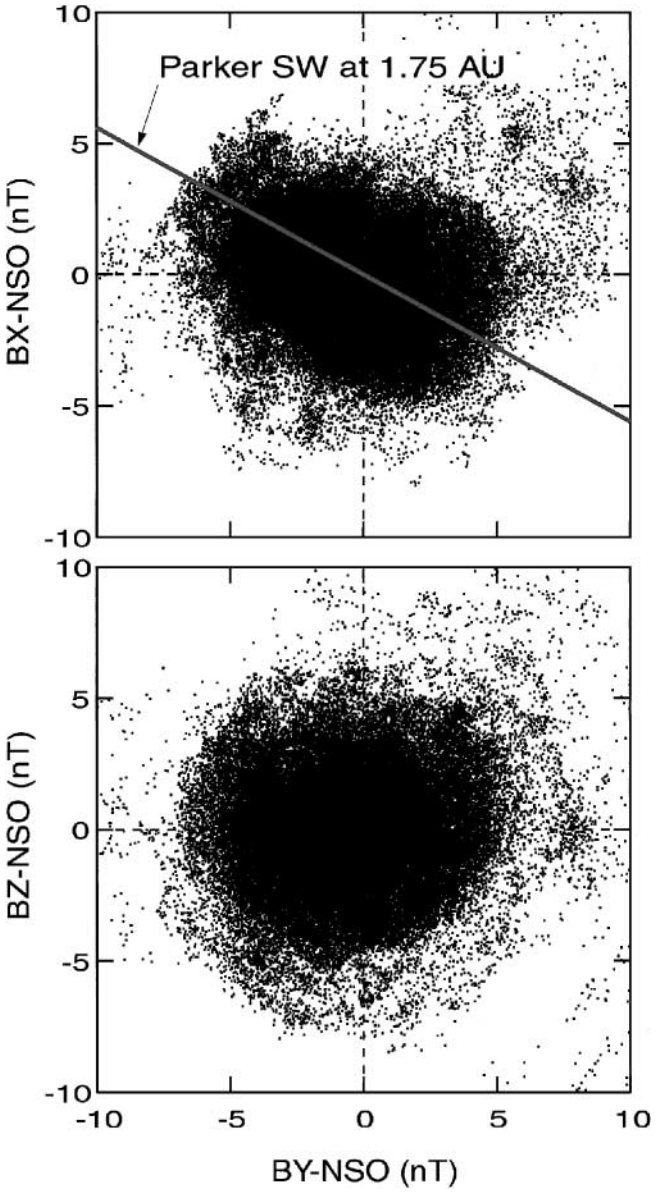

FIG. 1. Scatter plot of magnetic field data acquired in the 50-km-radius orbit in NSO coordinates. The points represent 1-min averages of data acquired from 30 April through 7 July 2000. The correlation between the *BX* and *BY* data corresponds to that expected for the interplanetary magnetic field at the orbit of 433 Eros during this epoch, 1.75 AU, and no signature due to the presence of an asteroidal field is found.

demagnetization factors. Thus, a significant "global" magnetic field is unlikely to exist. Differentiated meteorites, which have experienced partial melting and separation of materials according to density, generally exhibit Fe-rich concentrations of materials (Feierberg *et al*. 1982, Gaffey *et al*. 1993) with significant thermo-remanent magnetization (TRM). The detection of a global magnetic field at 433 Eros would have immediately established it as a differentiated asteroid with Fe-rich mass concentrations, supporting theoretical speculations about early igneous differentiation of planetary bodies (Gaffey *et al*. 1993).

2. INSTRUMENTATION AND DATA

The NEAR-Shoemaker magnetometer instrument was built as a cooperative undertaking between the Laboratory for Extraterrestrial Physics of NASA's Goddard Space Flight Center and the Space Department of the John Hopkins University Applied Physics Laboratory. A full description of this instrument and its calibration have been given in Acuña *et al*. (1997) and Lohr *et al*. (1997). The calibration in flight to identify and develop procedures to remove magnetic fields due to the spacecraft in ground processing are described in Anderson *et al*. (2001).

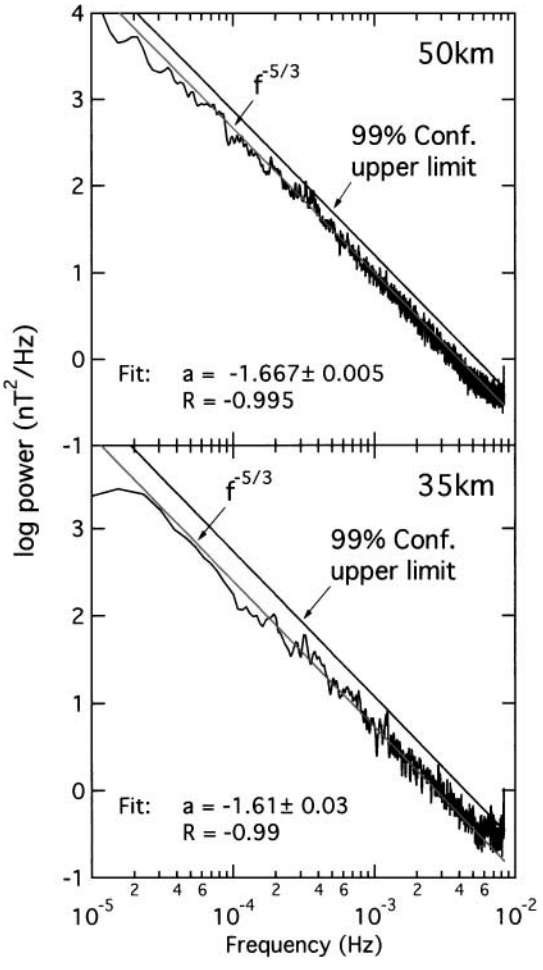

FIG. 2. Search for an Eros-rotation-induced signature in the magnetic field data. Plots show the trace of the spectral matrix evaluated for all three components of the field. The 35-km orbit spectrum is an average of four spectra of consecutive 36-h intervals of 1-min averages of data from 14 to 24 July 2000. The 50-km orbit spectrum is an average of 11 spectra of consecutive 144-h intervals of 1-min averages of data from 30 April through 7 July 2000. Both epochs yield nearly equal spectral indexes of $-5/3$, which is indicative of typical IMF fluctuations. The solid lines above the power spectra indicate the 99% confidence level upper limit for signals relative to the $f^{-5/3}$ spectrum (Bendat and Piersol 1986). There are no discernible low-frequency peaks above the 99% confidence level corresponding to the combined effects of the spacecraft orbital period (20 h or 1.4×10^{-5} Hz) in the 35-km orbit or (30 h or 9.3×10^{-6} Hz) in the 50-km orbit. The asteroid rotation period is 5.27 h or 5.3×10^{-5} Hz.

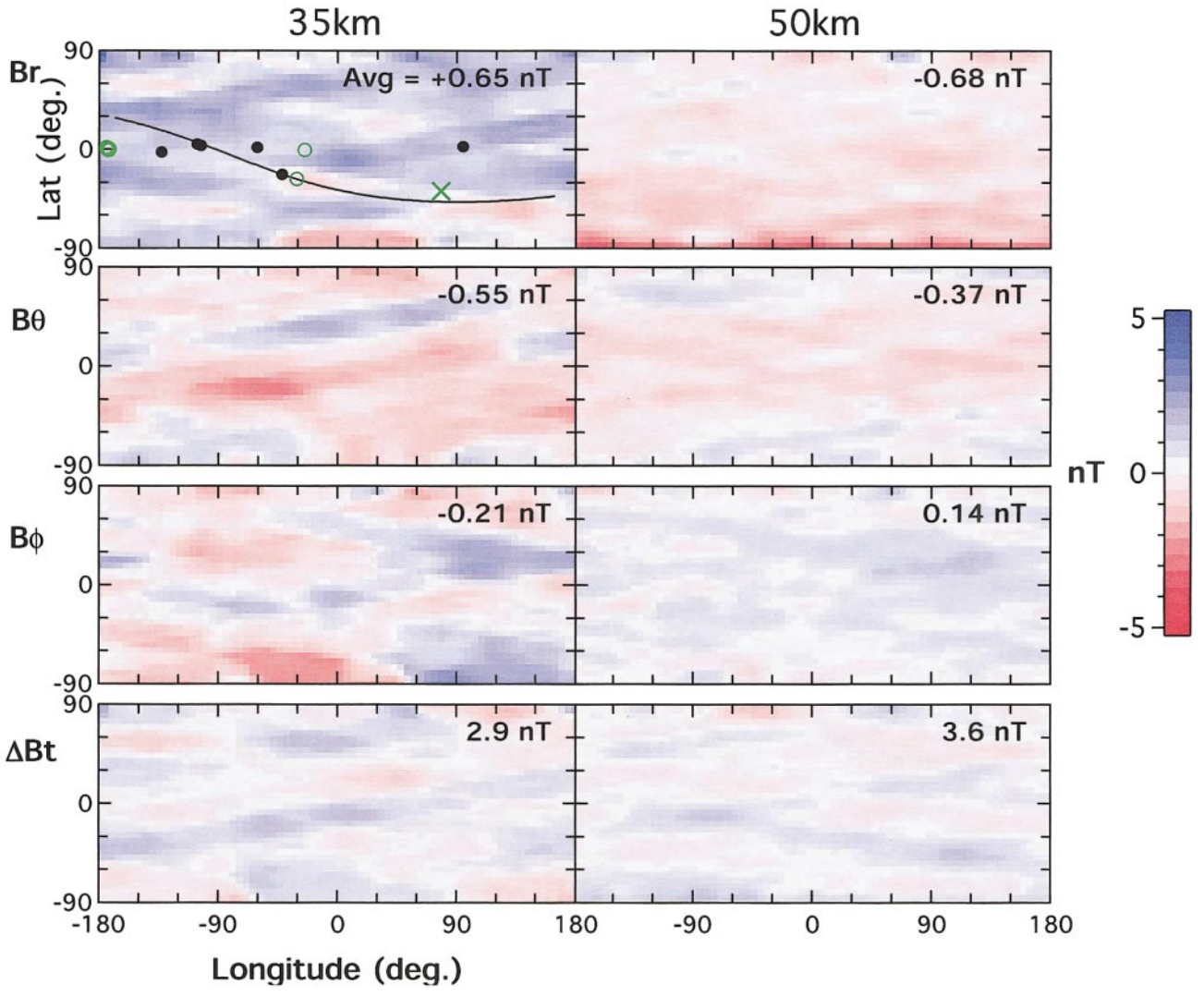

FIG. 3. Magnetic field maps of data acquired from the 35-km-radius orbit and 50-km-radius orbit in Eros-body-fixed (EBF) spherical polar coordinates B_r, B_θ, and B_ϕ. The total field magnitude B_t is illustrated in the bottom panel by showing the residuals, δB_t, from the average B_t. The presence of a dipolar field should show two hemispheres with oppositely directed radial fields and the polar and azimuthal components would show banded structures with one to four bands depending on the orientation of the field. There is no signature of a dipole field at a level of $\sim$1 nT. The average radial field at 35 km is 0.7 nT and indicates an intrinsic error limit in the data of 0.5 to 1 nT. Symbols in the upper left panel show locations of minimum Eros-centric distances (black circles), minimum distance from the surface (green circles), track of the 26 October 2000 flyover (black trace), and the landing site (green X). Tracks for the low-altitude flyovers of January 2001 all occurred within $\pm 5^\circ$ latitude.

The basic instrument configuration consists of a single, wide-range, triaxial fluxgate sensor mounted on the spacecraft antenna feed support structure. This arrangement, although not optimum for high sensitivity or weak field measurements, was considered adequate for the more focused objectives of a Discovery-class mission. Implementation of this experiment without stringent spacecraft magnetics controls (which usually includes a long deployable boom) lowered the cost of accommodation requirements and the total spacecraft mass at the expense of a more complex data reduction effort on the ground. The latter introduces moderate but tolerable increases in measurement uncertainty (Anderson *et al.* 2001). The NEAR magnetometer is capable of operating over a large dynamic range of field measurement capability, from ± 4 nT to $\pm 65{,}536$ nT full scale in eight automatically selected ranges. Three 20-bit, sigma-delta A/D converters are used to digitize the internal data at a rate of 20 samples/s and provide input to digital filters which include high-pass (AC) channels for the detection of high-frequency fluctuations. The measurement resolution transmitted to the ground is 16 bits for the DC and low-frequency magnetic field data and 8 bits logarithmic for the AC channel outputs. As described in Anderson *et al.* (2001), the sampling rate for the magnetometer was commandable from 0.6 bits per second (bps) to 1200 bps, corresponding to 0.01 to 20 sample/s, respectively. In addition, the valid science

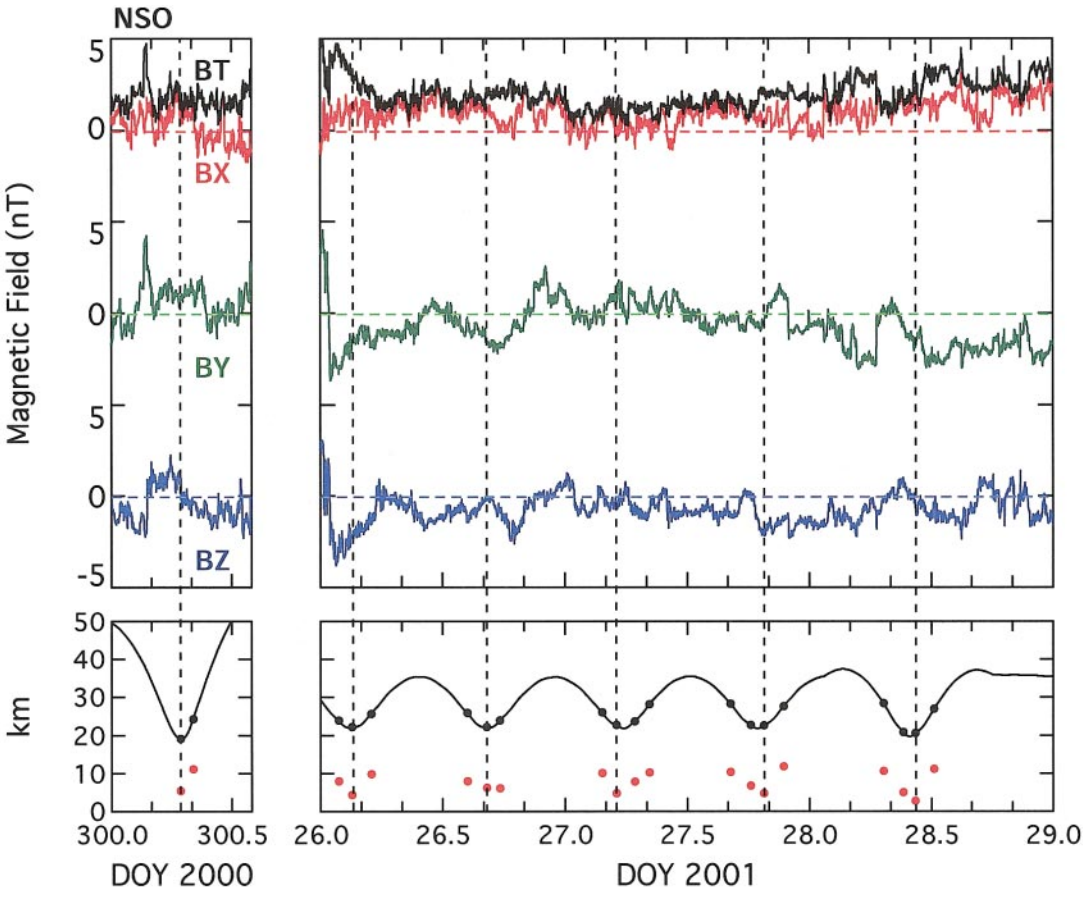

FIG. 4. The left-hand panels illustrate the data acquired on 26 October 2000 during a close flyby of Eros in NSO coordinates. The right-hand panels show similar data acquired during the 26–29 January 2001 time period. Black and red dots in the bottom panels show the Eros-centric distance and minimum altitude, respectively, for minimum altitudes below 6 km. Data from the single pass on 26 October appear to suggest the presence of an asteroidal field but the repeated orbital sampling provided by NEAR demonstrates that the observed signature is simply associated with typical variations of the interplanetary magnetic field.

data are only obtained when spacecraft housekeeping data are available and the spacecraft housekeeping rate was also variable. During rendezvous the magnetometer was operated at a sample rate of 1 sample/s and the spacecraft housekeeping rate was typically 1 sample every 10 s. The resulting magnetometer sampling interval for magnetometer science data during rendezvous was 10 s.

The NEAR-Shoemaker spacecraft was inserted initially into a nearly circular 200-km orbit around Eros and subsequent orbit adjustments brought the spacecraft to orbits of 100-, 50-, and 35-km nominal radii with respect to Eros' center of mass (Cheng 1997). The spacecraft made close flyby passes of the asteroid, with closest approach distances as low as 2.7 km from the surface, and eventually landed on Eros on 12 February 2001, remaining operational for approximately two weeks. NEAR-Shoemaker is the first spacecraft to have conducted magnetic field measurements from orbit around an asteroid and from its surface. We report here results obtained from 50- and 35-km-radius orbits, from the close approach at 15 km from the center of mass, and from the measurements carried out on Eros' surface after landing. In-flight calibration data taken during cruise from April 1996 to February 2000 revealed the existence of significant offset fields produced by the spacecraft, which were very steady and therefore removable (Anderson *et al*. 2001). Other spacecraft-induced fields from various current loops produced fields at the sensor on the order of 5 nT each. These perturbations were associated with spacecraft engineering systems, and telemetery information from current monitors was used to develop a general spacecraft magnetic field model to remove the resulting dynamic signatures from the data. Cross-correlations with magnetic field data from the WIND and ACE spacecraft were conducted as independent verification of the spacecraft magnetic field model and NEAR-Shoemaker calibration activities with excellent results (Anderson *et al*. 2001). The accuracy of the magnetic field data, corrected for spacecraft induced fields, is of the order of $\sim$1 nT (Anderson *et al*. 2001). Reconfiguration of spacecraft subsystems in preparation for landing resulted in additional disturbances including undetermined effects after

landing which increased the measurement bias uncertainty associated with data acquired from the surface to ∼5 nT.

Two coordinate systems are used to analyze the data, NEAR-Sun-orbital (NSO) and Eros-body-fixed (EBF). NSO coordinates are Cartesian coordinates defined with respect to the NEAR–Sun line and the orbit plane of 433 Eros. The x axis points from NEAR to the Sun, the y axis is parallel to the 433 Eros orbital plane and is defined positive in the opposite direction to the velocity vector. The z axis completes the right-handed triad, pointing in the general direction of the northern ecliptic plane. EBF coordinates are spherical polar coordinates defined, with the radius measured from Eros' center-of-mass, as follows: B_r is directed radially outward, B_θ is defined positive south along the local meridian, and B_ϕ is defined positive east along the local parallel.

3. EROS 433 ORBITAL OBSERVATIONS

The magnetic field at NEAR-Shoemaker was continuously monitored during the approach to Eros from April 1999 through orbit insertion on 14 February 2000, over distances from >100,000 km to 400 km from Eros, and no signatures distinct from interplanetary magnetic fields (IMF) were observed. Immediately after Eros orbit insertion, magnetic perturbations in the apparent vicinity of the asteroid were detected, but these were later shown to be of IMF origin. Scatter plots of the magnetic field data obtained in the 50-km orbit plotted in NSO coordinates are shown in Fig. 1. No coherent pattern is found other than that associated with the expected IMF "Parker spiral" angle at 1.75 AU, corresponding to Eros' distance to the Sun during the 50-km orbit epoch, and illustrated by the straight line in the upper panel. The interplanetary magnetic field geometry, when viewed from above the ecliptic plane, resembles that of an Archimedean spiral centered at the Sun. The angle that the magnetic field line forms with the Earth–Sun line at 1 AU is on the average ∼45°, but significant variability is observed. At the orbit of 433 Eros (1.75 AU) this angle increases to ∼61°. The 50- and 35-km orbit radii are significantly smaller than the typical proton gyro-radius at 1.75 AU and no large-scale perturbations of the IMF are expected (and none are seen) if the solar wind interaction with Eros involves an unmagnetized or weakly magnetized body.

Figure 2 shows the results of spectral analyses performed on the 50- and 35-km orbit data to search for a possible signature at frequencies related to Eros rotation, 5 h 17 m in period or 5.258×10^{-5} Hz. The slope of the power spectral density curve corresponds to that expected for the IMF ($\sim f^{-5/3}$), as indicated by the line fit to the spectra drawn in the figure. The solid lines above the power spectra indicate the 99% confidence level upper limit for signals relative to the $f^{-5/3}$ spectrum (Bendat and Piersol 1986). The 35-km and 50-km spectra were evaluated by averaging 4 and 11 spectra, respectively. Since each spectrum is the trace of a 3×3 spectral matrix, the spectral estimates correspond to 12 and 33 degrees of freedom for the 35-km and 50-km data respectively.

No signals at Eros' rotation rate or its harmonics are found above the 99% upper limits. The strongest signals from a dipole magnetic field would appear at frequencies corresponding to twice the Eros rotation rate, or near 0.1 mHz. At this frequency the upper limit log power of the 35-km orbit data is $630\ \mathrm{nT}^2 \cdot \mathrm{Hz}^{-1}$. The bandwidth of the Hamming window used to process these data is 0.017 mHz, so the rms magnetic signal amplitude upper limit is ∼0.1 nT.

The data acquired from the 35- and 50-km orbits have been plotted in EBF coordinates and are shown as magnetic field maps in Fig. 3 together with locations of flyover minimum approach distances and the landing site. The plots show a map of the averaged spherical polar components of the magnetic field in EBF coordinates plus the total field magnitude. Bins without data were filled with median values of nearest neighbors having data. Data were then smoothed by averaging over areas of 5×5 bins ($25^\circ \times 25^\circ$). Sloping striations reflect the spacecraft orbit and resulting pattern of data coverage. The observed variations in the magnitude of the ambient magnetic field components are uncorrelated with Eros longitude and clearly of solar wind origin.

The left upper panel of Fig. 4 shows data acquired during the close approach pass on 26 October 2000 as magnetic field components (*BX, BY, BZ*) and total field magnitude (*BT*) in NSO coordinates. The bottom left panel in the figure shows the corresponding radial distance from NEAR to Eros' center of mass. The right-hand panels illustrate, in the same format, data acquired during the 26–29 January 2001 time period while the spacecraft orbited Eros at close-in range. The variability of the measured field is typical of the IMF and no Eros correlated signature is observed. It is interesting to note that the data from the single pass on 26 October 2000 (*BY* and *BZ* components) could be construed as suggesting the presence of a weak asteroidal field. However, the repeated orbital sampling provided by NEAR-Shoemaker unambiguously disproves such a suggestion.

4. DESCENT AND SURFACE OBSERVATIONS

On 12 February 2001 the spacecraft was placed on an Eros-landing trajectory using its onboard thrusters to reduce the approach velocity and achieve a "soft" landing in an area south of Himeros, the saddle-shaped depression on Eros located at ∼15°N, 280°W. Remarkably, the spacecraft remained functional after the landing and the magnetic field instrument was activated, acquiring data from Eros' surface for ∼2 h on 15 February and ∼1.2 h on 18 February. The landing approach data are shown in Fig. 5. The three components of the magnetic field and its magnitude are shown in two coordinate systems, EBF and NSO, with the bottom panel illustrating the radial distance to Eros as a function of time. There is no indication of any gradual increase in the measured field prior to 18:00 UT as the spacecraft approaches the surface, as would be expected if Eros were a magnetized body. Spacecraft reconfiguration and thruster activity prior to landing are evident in the data as increased high-frequency "noise" and

sudden jumps in the measured field values. Landing occurs at ~19:42 UT when magnetometer data are no longer transmitted to Earth.

These results are consistent with magnetic field observations during close flybys of the asteroid. The data acquired on the surface of Eros are shown in Fig. 6 and once more are representative of interplanetary magnetic field values and variability. The increased uncertainty associated with the surface measurements place an upper limit of ~5 nT on a possible asteroidal field at the landing site. Eros is therefore a remarkably nonmagnetic object. Spacecraft housekeeping data indicate that the solar panels generated slightly less current after landing than would have been expected. This is consistent with the loss of function of cells at the ends of the panels in contact with the asteroid. It is not known whether this is due to damage, partial burial in the regolith, or coverage by dust. Since opposite solar panels generate cancelling magnetic fields (Anderson *et al*. 2001), the loss of power from the ends of two panels could account for the observed ~5 nT fixed offset magnetic field. We therefore find no evidence for a magnetic field at the surface.

5. EROS 433 MAGNETIZATION UPPER LIMIT

During the orbital mission the spacecraft came as close as 2.7 km above the surface of Eros. Rough estimates of the global magnetic moment required to produce a 1-nT field at the NEAR magnetometer sensor location can be made assuming that the putative point source is located at 2.7 km from the measurement position. The value derived for the global natural remanent magnetization (NRM) dipole moment under the 2.7-km assumption is extremely low, $\lesssim 2 \times 10^8$ A · m^2. An estimate for the globally averaged magnetization is provided by the 35-km orbit data. Using the 0.1-nT upper limit obtained from the 35-km orbit data, the upper limit magnetization moment is $<4.3 \times 10^{10}$ A · m^2.

To obtain a more precise estimate for an upper limit to the global, uniform magnetization of Eros, we used an axisymmetric, finite element model of Eros to estimate the maximum magnetization per unit volume consistent with the upper limit of ~5 nT at the landing site. The computer software used for the numerical simulations was FEMM 2.1 (a), a freely available, finite element magnetics modeling program developed by D. Meeker (http://hometown.aol.com/qmagnetics/download.htm). A uniform volume magnetization in excess of ~0.005 A · m^{-1}, in any direction, would exceed the detection threshold (~5 nT) established here. Using accepted values of mass and volume for 433 Eros, 6.69×10^{15} kg (Yeomans *et al*. 2000) and 2.50×10^{12} m^3 (Zuber *et al*. 2000, Thomas *et al*. 2000), the corresponding upper limit to the total remanent magnetic moment for the asteroid is $<1.3 \times 10^{10}$ A · m^2. This is about a factor of 3 lower than that obtained from the 35-km orbit data, reflecting the enhanced sensitivity to a global magnetization from the surface relative to orbit, which more than offsets the coarser detection level achieved at the surface. This value yields a maximum NRM · kg^{-1} for Eros of $<1.9 \times 10^{-6}$ A · m^2 · kg^{-1}, which we adopt as an upper limit value for Eros.

6. DISCUSSION

An important objective of the NEAR mission was to determine if 433 Eros was magnetized to the level inferred for Gaspra, another S-type asteroid, based on Galileo observations of large-scale perturbation of the IMF (Kivelson *et al*. 1993). Recently, Richter *et al*. (2001) have also reported on observations acquired on a flyby of Asteroid Braille by the DS-1 spacecraft and argued for a high level of intrinsic magnetization for this asteroid. Clearly, the results reported here and obtained from direct *in situ* measurements, without ambiguity, pose new and challenging questions about these interpretations and the generic association of S-class asteroids with possible intrinsic magnetization. The S class of asteroids is the most extensively subdivided of all the asteroid classes and Braille and Gaspra could simply be quite different from Eros, either in metamorphic or collisional history, or in both. It is also important to emphasize that the difficulties associated with distinguishing extremely weak asteroidal fields from the much larger and variable interplanetary magnetic field may contribute significantly to this apparent interpretation conflict.

Following the work of Sugiura and Strangway (1988) we show in Fig. 7 the range of upper limits derived for Eros' magnetization against ordinary chondrites and E chondrites, as a function of saturation isothermal remanent magnetization per kilogram (SIRM). Assuming that the bulk magnetization is due to a uniform magnetization of the asteroid material, the magnetic observations support the interpretation of Eros as a primitive, undifferentiated body within the approximate class of LL chondrites. Ordinary chondritic meteorites are classified according to their composition and iron content into the classes H, L, and LL, with LL having the least amount of total iron and metal content. This is consistent with independent interpretations derived from gravity data (Yeomans *et al*. 2000) and X-ray fluorescence studies (Trombka *et al*. 2000).

Observationally, the low global magnetization state of chondrites is attributed to their being composed of individual components (chondrules, metal grains, and matrix), which independently may exhibit much higher magnetization states but are assembled with their magnetic moments randomly oriented so that the average moment of the body as a whole is much smaller than the small-scale magnetization (Morden and Collinson 1992). Hence, it is important to establish, in addition to an upper limit to the global magnetization state of Eros, an upper limit to any detectable magnetization state associated with identifiable small-scale structures such as nearby boulders. Since the origin or process of formation of the latter are not known, an estimate of the detectable magnetization state is important to rule out possible extra-Eros sources. The images acquired by the NEAR-Shoemaker spacecraft during the low-altitude flyovers (Veverka *et al*. 2000) reveal the existence of numerous meter-sized boulders at the surface. Imaging along the landing trajectory and within 120 m of the surface show the presence of several meter-size, boulder-like structures near the landing site (Veverka *et al*. 2001). Although the exact position of the

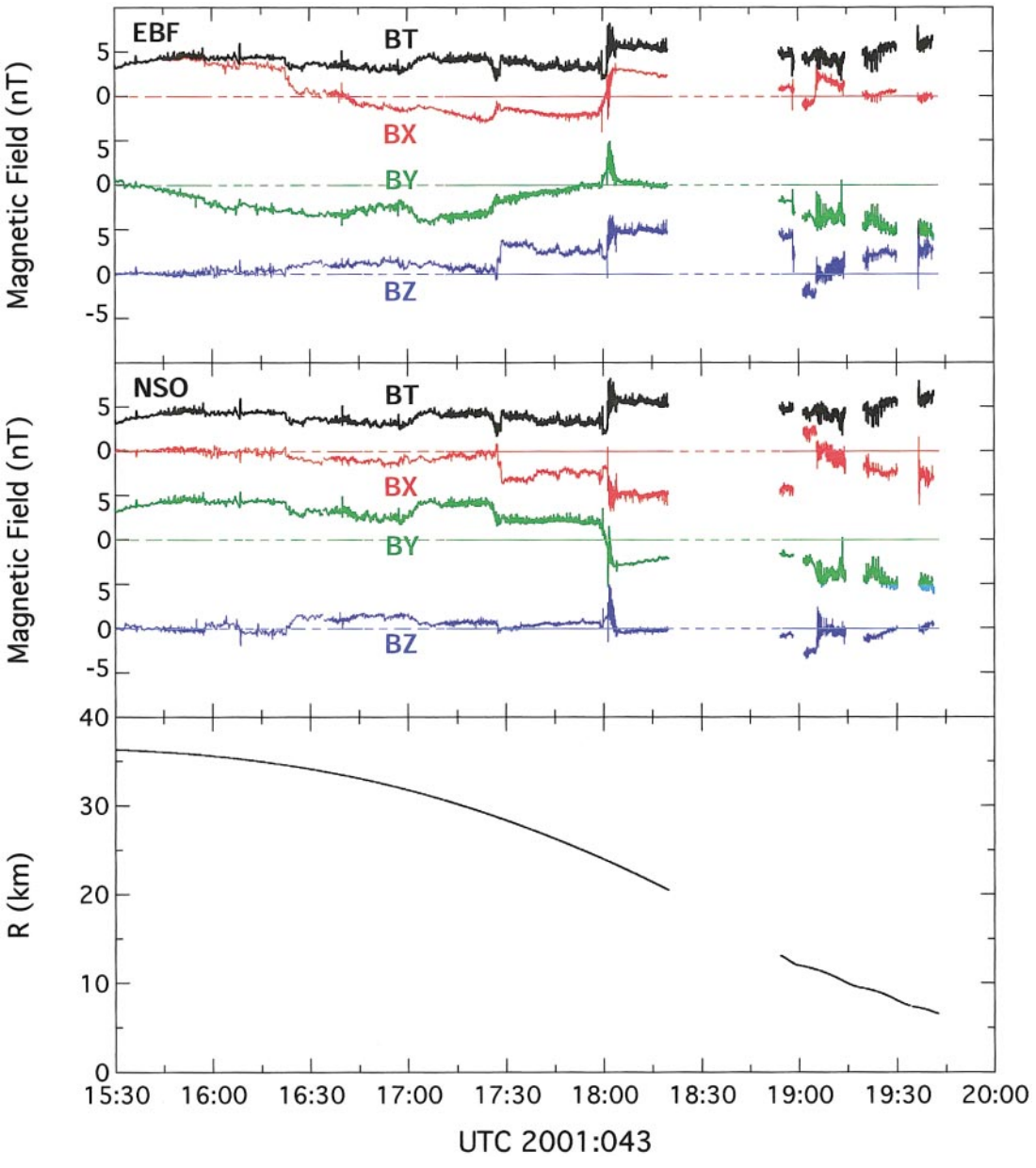

FIG. 5. Magnetic field data acquired during the descent to 433 Eros on 12 February 2001 in EBF and NSO coordinates (7). The radial distance from the spacecraft to the center of mass is shown in the bottom panel. Prior to 18:00 UT the data reflect typical signatures associated with the IMF. At this time the spacecraft is reconfigured for landing, resulting in increased perturbations and abrupt jumps in the measured field components. The data have been corrected for known spacecraft effects to a level of ~5 nT. There is no noticeable increase in the measured field magnitude as the spacecraft approaches the asteroid.

spacecraft with respect to these structures is unknown we can estimate the magnetization per unit volume required to generate a field of ~5 nT at the spacecraft location by a 4-m diameter boulder located 10 m away as ~1.2–2.3 $A \cdot m^{-1}$ (4.5×10^{-4} to 9×10^{-4} $A \cdot m^2 \cdot kg^{-1}$) depending on orientation. If, however, the edge of the same boulder is located 3 m away from the spacecraft this values is reduced to ~0.1 to 0.2 $A \cdot m^{-1}$ (3.7×10^{-5} to 7.4×10^{-5} $A \cdot m^2 \cdot kg^{-1}$). Both values are significantly larger than those estimated for the bulk magnetization state of 433 Eros (<0.005 $A \cdot m^{-1}$—see previous section) since the assumed volume for the purported boulder is far smaller than the entire asteroid. Previous laboratory studies of meteorites identified randomness in the magnetization measured in subsamples removed with mutual orientation intact from the ordinary chondrites (Morden and Collinson 1992). This work was extended by P. Wasilewski *et al*. (private communication) to larger objects in anticipation of the NEAR mission, but no access to magnetic measurements of several-meter- and kilometer-size objects was possible. Therefore, the NEAR observations place new constraints on possible relations between NRM and object size.

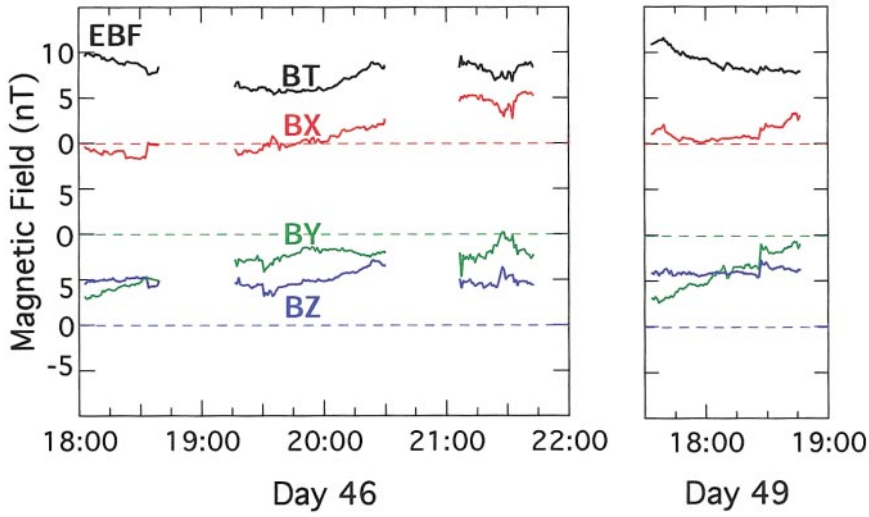

FIG. 6. On 15 February 2001 after the successful landing, the NEAR magnetic field experiment was activated and data were acquired for the time intervals and dates illustrated. A bias of 5–8 nT in the spacecraft reference frame is probably associated with shadowing or partial burial of the solar array after landing. The estimated detection uncertainty for a magnetic field due to Eros is ∼5 nT. The observed signatures are consistent with IMF variability.

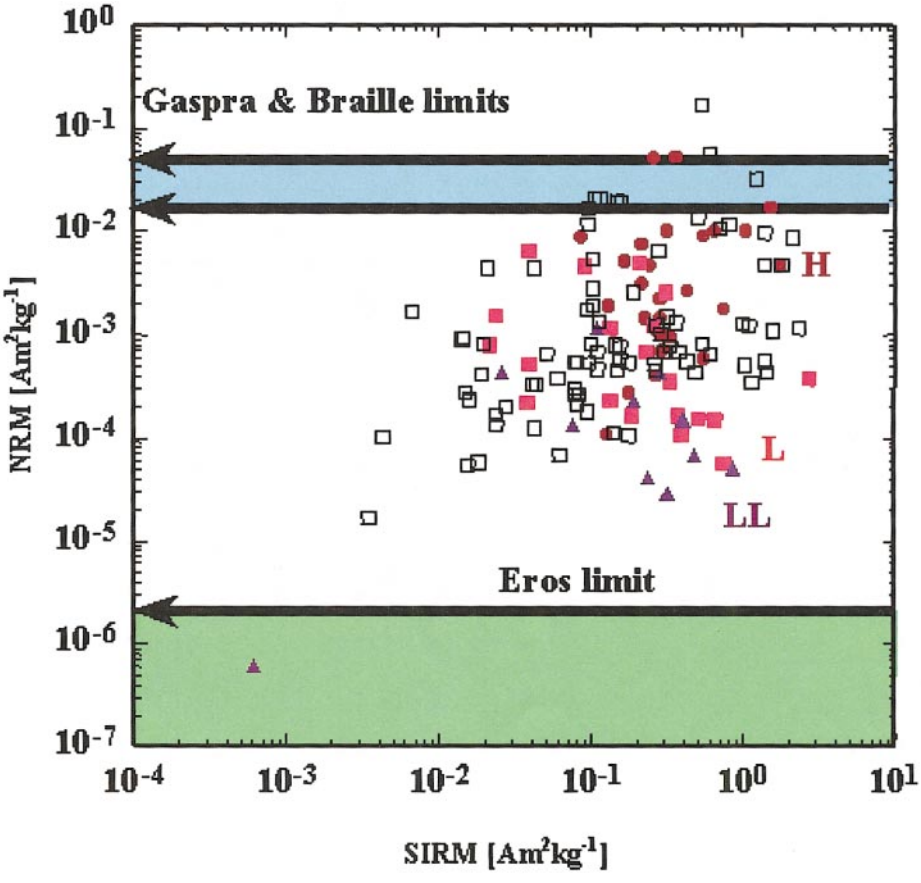

FIG. 7. Plot of NRM vs SIRM for H (solid circles), L (solid squares), and LL (solid triangles) chondritic meteorites, (13, 17) together with the magnetization of chondrules from the Bjurbole (L4) meteorite (empty squares). The upper limit derived for 433 Eros is shown as a solid band below 1.9×10^{-6} A · m^2 · kg^{-1}, illustrating its chondritic and remarkably nonmagnetic character.

It is clear that the NEAR-Shoemaker magnetic field measurements reflect only the present state of the asteroid and do not resolve the critical question of Eros metamorphic or collisional history and its implications for the origin and evolution of S-class asteroids. Future progress in this area must rely on further analysis and interpretation of interdisciplinary NEAR data, including gravity, gamma-ray, and X-ray data sets, as well as additional ground- and space-based measurements. Recent advances in the study of the martian and lunar paleo-fields may prove to be of significant relevance to the understanding of Eros' current magnetization state and its origin.

ACKNOWLEDGMENTS

We thank the NEAR Project at Johns Hopkins University/Applied Physics Laboratory (JHU/APL) for the support provided to the magnetic field investigation. We also thank the NEAR engineering team for supporting the acquisition of data to allow the correction of spacecraft-induced fields. The contributions of Dave Lohr at JHU/APL and J. Scheifele, Maria Kirsch, and Everett Worley at the Goddard Space Flight Center are gratefully acknowledged.

REFERENCES

Acuña, M. H., C. T. Russell, L. J. Zanetti, and B. J. Anderson 1997. The NEAR magnetic field investigation: Science objectives at Asteroid Eros 433 and experimental approach. *J. Geophys. Res.* **102**, 23751–23759.

Anderson, B. J., L. J. Zanetti, D. A. Lohr, J. R. Hayes, M. H. Acuña, C. T. Russell, and T. Mulligan 2001. In-flight calibration of the NEAR magnetometer. *IEEE Trans. Geosci. Remote Sensing* **39**, 907–917.

Bendat, J. S., and A. G. Piersol, 1986. *Random Data, Analysis and Measurement Procedures*, 2nd ed. Wiley, New York.

Cheng, A. F. 1997. Near Earth Asteroid Rendezvous: Mission overview. *Space Sci. Rev.* **82**(1–2), 3–29.

Feierberg, M. A., H. P. Larson, and C. R. Clark 1982. Spectroscopic evidence for undifferentiated S-type asteroids. *Astrophys J.* **257**, 361–372.

Gaffey, M. J., T. H. Burbine, and R. P. Binzel 1993. Asteroid spectroscopy–Progress and perspectives. *Meteoritics* **28**, 161–187.

Kivelson, M. G., L. F. Bargatze, K. K. Khurana, D. J. Southwood, R. J. Walker, and P. J. Coleman Jr. 1993. Magnetic field signatures near Galileo's closest approach to Gaspra. *Science* **271**, 331–334.

Lohr, D. A., L. J. Zanetti, B. J. Anderson, T. A. Potemra, J. R. Hayes, R. E. Gold, R. M. Henshaw, F. F. Mobley, D. B. Holland, M. H. Acuña, and J. L. Scheifele 1997. Near magnetic field investigation, instrumentation, spacecraft magnetics and data access. *Space Sci. Rev.* **82**(1–2), 255–281.

Morden, S. J., and D. W. Collinson 1992. The implications of the magnetism of ordinary chondrite meteorites. *Earth Planet. Sci. Lett.* **109**, 185–204.

Richter, I., D. E. Brinza, M. Cassel, K.-H. Glassmeier, F. Kuhnke, G. Musmann, C. Ohtmer, K. Schwingenschuh, and B. T. Tsurutani 2001. First direct magnetic field measurements of an asteroidal magnetic field: DS1 at Braille. *Geophys. Res. Lett.* **28**(10), 1913–1916.

Sugiura, N., and D. W. Strangway, 1988. Magnetic studies of meteorites. In *Meteorites and the Early Solar System* (J. F. Kerridge and M. S. Matthews, Eds.), pp. 595–615. Univ. Arizona Press, Tucson.

Thomas, P. C., J. Joseph, B. Carcich, B. E. Clark, J. Veverka, J. K. Miller, W. Owen, B. Williams, and M. Robinson 2000. The shape of Eros from NEAR imaging data. *Icarus* **145**, 348–350.

Trombka, J. I., S. W. Squyres, J. Bruckner, W. V. Boynton, R. C. Reedy, T. J. McCoy, P. Gorenstein, L. G. Evans, J. R. Arnold, R. D. Starr, L. R. Nittler, M. E. Murphy, I. Mikheeva, R. L. McNutt Jr., T. P. McClanahan, E. McCartney, J. O. Goldsten, R. E. Gold, S. R. Floyd, P. E. Clark, T. H. Burbine, J. S. Bhangoo, S. H. Bailey, and M. Petaev 2000. The elemental composition of Asteroid 433 Eros: Results of the NEAR-Shoemaker X-ray spectrometer. *Science* **289**, 2101–2105.

Veverka, J., P. C. Thomas, M. Robinson, S. Murchie, C. Chapman, M. Bell, A. Harch, W. J. Merline, J. F. Bell, B. Bussey, B. Carcich, A. Cheng, B. Clark, D. Domingue, D. Dunham, R. Farquhar, M. J., Gaffey, E. Hawkins, N. Izenberg, J. Joseph, R. Kirk, H. Li, P. Lucey, M. Malin, L. McFadden, J. K. Miller, W. M. Owen, C. Peterson, L. Prockter, J. Warren, D. Wellnitz, B. G. Williams, and D. K. Yeomans 2000. Imaging of small-scale features on 433 Eros from NEAR: Evidence for a complex regolith. *Science* **292**, 484–488.

Veverka, J., R. Farquhar, M. Robinson, P. Thomas, S. Murchie, A. Harch, P. G. Antreasian, S. R. Chesley, J. K. Miller, W. M. Owen Jr., B. G. Williams, D. Yeomans, D. Dunham, G. Heyler, M. Holdridge, R. L. Nelson, K. E. Whittenburg, J. C. Ray, B. Carchich, A. Cheng, C. Chapman, J. F. Bell III., M. Bell, B. Bussey, B. Clark, D. Domingue, M. J. Gaffey, E. Hawkins, N. Izenberg, J. Joseph, R. Kirk, P. Lucey, M. Malin, L. McFadden, W. J. Merline, C. Peterson, L. Prockter, J. Warren, and D. Wellnitz 2001. The landing of the NEAR-Shoemaker spacecraft on Asteroid 433 Eros. *Nature* **413**, 390–393.

Wasson, J. T., and G. W. Wetherill 1979. Dynamical chemical and isotopic evidence regarding the formation locations of asteroids and meteorites. In *Asteroids* (T. Gehrels, Ed.), pp. 926–974. Univ. of Arizona Press, Tucson.

Yeomans, D. K., P. G. Antreasin, J.-P. Barriot, S. R. Chesley, D. W. Dunham, R. W. Farquhar, J. D. Giorgini, C. E. Helfrich, A. S. Konopliv, J. V. McAdams, J. K. Miller, W. M. Owen Jr., D. J. Scheeres, P. C. Thomas, J. Veverka, B. G. Williams 2000. Radio science results during the NEAR-Shoemaker spacecraft rendezvous with Eros. *Science* **289**, 2085–2088.

Zuber, M. T., D. E. Smith, A. F. Cheng, J. B. Garvin, O. Aharonson, T. D. Cole, P. J. Dunn, Y. Guo, F. G. Lemoine, G. A. Neumann, D. D. Rowlands, and M. H. Torrence 2000. The shape of 433 Eros from the NEAR-Shoemaker laser rangefinder. *Science* **289**, 2097–2101.